2.1 μm Band Dissipative Soliton Resonance Mode-Locked Ho-Doped Tunable Fiber Laser

Xin Li, Tianshu Wang, Wanzhuo Ma, Lei Du, Hang Ren, and Lin Xiao

***Abstract*—We report a 2.1 μm band mode-locked holmium-doped fiber (HDF) laser with tunable wavelength and pulse width in dissipative soliton resonance (DSR) region for the first time to our knowledge. A piece of HDF is pumped by a home-made 1.9 μm band fiber source, and a nonlinear-amplifying-loop-mirror structure is used to realize mode-locking operation with net anomalous dispersion. The repetition rate of pulse is 8.97 MHz. The pulse duration can be adjusted from 1.16 to 3.93 ns with the increase of pump power, while maintains a constant peak power. At the maximum pump power of 2.1 W, the pulse energy is up to 2 nJ. Moreover, the central wavelength is in the tunable range from 2054.4 to 2076 nm by appropriately adjusting the polarization controllers. We also explore the nonlinear correlation characteristic of DSR pulse by changing the length of high nonlinear fiber.**

***Index Terms*—Mode-locked laser, holmium-doped fiber laser, dissipative soliton resonance, wavelength-tunable.**

I. Introduction

RECENTLY, 2 μm band mode-locked fiber lasers have become a topic of extensive concern and widely used in a variety of research fields, including free-space optical communication, polymer welding, medical surgery and pump source of mid-infrared optical parametric oscillators, etc. [1]–[5]. However, most of optical fibers have large anomalous dispersion in the 2 μm band [6], [7], hence the solitons can be actually formed in a non-dissipative system [8]. The pump power is too high to hold on one soliton in quantity according to the theory of soliton area. Therefore, the single pulse usually can bear lower energy in some extent [9], [10].

In 2008, Chang et al. theoretically proposed a novel soliton operation state based on the numerical solution of the complex cubic-quantic Ginsburg-Landau equation, dissipative soliton resonance (DSR) pulse [11]. The pulse profile of DSR is rectangular. It is different from conventional soliton lasers, the duration and energy of DSR pulse can increase monotonously and limitlessly with the increase of pump power without wave-breaking, whilst the peak power is almost unchanged [12]–[14]. Thus, DSR pulse is expected to be nanosecond square-wave pulses with high pulse energy in a mode-locked laser cavity.

For another, mode-locked fiber lasers with tunable or switchable wavelength have aroused much concern recently. There are wide range of applications, such as pump-probe microscopy and coherent Raman scattering imaging [15]–[18]. However, most of DSR fiber lasers are concentrated in ytterbium-doped fiber laser (YDFL) and erbium-doped fiber laser (EDFL) operating at the 1 μm [19] and 1.55 μm [20], [21]. As far as we know, the largest spectral range for the 1 μm band DSR mode-locked fiber laser without any other intra-cavity filtering mechanism is 38 nm [22]. In 2020, a YDFL with wavelength-tunable range of 73 nm (from 1007 to 1080 nm) was further obtained by adding the intracavity filter [23]. For 1.55 μm band, Shuailin Liu et al. obtained 4 kinds of switched DSR states with center wavelength of 1572 nm, 1585 nm, 1590 nm and 1605 nm [24]. So far, the wavelength-switching or tunable DSR lasers at 2 μm band are relatively new [25], [26]. In 2015, Yi Xu et al. reported a thulium-doped fiber laser (TDFL) with center wavelength of 28.95 nm tunable range (1940.22-1969.17 nm) [27]. Although there have been many studies on fiber lasers operating in the DSR region, there is little relevant study in the DSR region over 2 μm. In 2018, Junqing Zhao et al. firstly demonstrated the DSR-like operation in mode-locked holmium-doped fiber laser (HDFL) by using a cascaded resonant pumping scheme in the anomalous dispersion region [28]. Next year, they also further obtained the DSR pulse and found that they can be converted into a burst emission pulse in the large normal dispersion region, which can enrich the dynamics of passively mode-locked fiber lasers [29]. In 2020, Zhao et al. further established a novel saturable absorber named nonlinear absorbing-loop mirror (NAbLM), which also realized DSR pulse [30].

In this letter, a DSR pulse with tunable wavelength and pulse duration operating at the 2.1 μm is demonstrated for the first time. A nonlinear-amplifying-loop-mirror (NALM) is employed as an artificial saturable absorber. When the DSR can operate at 2075.6 nm, the pulse width broadens from 1.16 to 3.93 ns as the pump power increases, and the peak power remains almost constant. In addition, the central wavelength has an adjustable range of 21.6 nm (2054.4 to 2076 nm) by appropriately adjusting

Manuscript received 6 May 2022; revised 5 June 2022; accepted 10 June 2022. Date of publication 16 June 2022; date of current version 17 August 2022. This work was supported in part by the National Natural Science Foundation of China under Grant 61975021 and 62005024, in part by the Natural Science Foundation of Jilin Province under Grants YDZJ202101ZYTS139 and 20200201263JC, in part by the Research Project of Jilin Provincial Education Department under Grant JJKH20210816KJ, and in part by Jilin Province Young Scientific and Technological Talents Supporting Project under Grant QT202104. *(Corresponding author: Tianshu Wang.)*

The authors are with the National and Local Joint Engineering Research Center of Space Optoelectronics Technology, Changchun University of Science and Technology, Changchun 130022, China, and also with the College of Opto-Electronic Engineering, Changchun University of Science and Technology, Changchun 130022, China (e-mail: 2020100294@mails.cust.edu.cn; wangts@cust.edu.cn; mawz@cust.edu.cn; 2020100233@mails.cust.edu.cn; 2020100277@mails.cust.edu.cn; 2020100212@mails.cust.edu.cn).

Digital Object Identifier 10.1109/JPHOT.2022.3182982

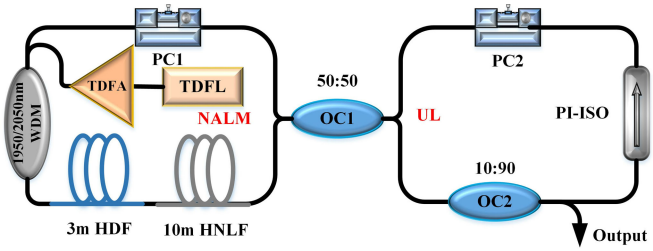

Fig. 1. Schematic diagram of the holmium-doped fiber laser. TDFL: thulium-doped fiber laser; TDFA: thulium-doped fiber amplifier; WDM: wavelength division multiplexer; HDF: holmium-doped fiber; HNLF: high nonlinear fiber; PI-ISO: polarization-independent isolator; PC: polarization controller; OC: optical coupler.

the orientation of the polarization controllers. When the pump power reaches a maximum of 2.1 W, the pulse energy is up to 2 nJ.

II. Experimental Setup

We construct a HDFL as shown in Fig. 1. The figure-eight resonator includes a standard NALM and a unidirectional loop (UL). As shown, the pump for a segment of 3 m holmium-doped fiber (Nufern, SM-HDF-10/130) is provided by a home-made TDFL fiber source at 1920 nm and power-boosted by a thulium-doped fiber amplifier (TDFA) with maximum pump power of 2.1 W. It is injected into the resonator through a 1950/2050 nm wavelength division multiplexer (WDM). A piece of 10 m high nonlinear fiber (HNLF) is used to accumulate phase shift for two opposite directions. Further employing a 50/50 optical coupler (OC), a NALM is established. On the both sides of the OC, a polarization controller (PC) is used to manipulate the intracavity polarization state, respectively, noted as PC1 and PC2. A unidirectional propagation loop is constituted by using polarization-independent isolator (PI-ISO). A 10/90 OC outputs 10% optical power. The total length of the laser is 23 m. All other fibers are standard SMF-28e. The laser operates in the negative dispersion region. The laser spectrum can be detected by an optical spectrum analyzer (YOKOGAWA, AQ6357). The pulse sequence and the radio frequency (RF) spectrum can be measured by a photodetector connected to a 2.5 GHz bandwidth oscilloscope (Agilent, DSO9254A) and a spectrum analyzer (Agilent, N1996A, 100 Hz-2.5 GHz), the long-term stability of the pulse is analyzed.

III. Experimental Results and Discussion

When the pump power reaches 589 mW, the experimental figure-eight fiber laser starts to output continuous wave. A stable mode-locking operation can be observed with proper rotation of the PC1 and PC2 at the pump power of 0.98 W and its characteristics are shown in Fig. 2. The smooth spectrum of DSR pulse with resolution of 0.02 nm at the maximum pump power of 2.1 W is shown in Fig. 2(a). The center wavelength is 2075.6 nm and the 3 dB bandwidth is about 5.43 nm. The typical DSR pulse is shown in Fig. 2(b), the pulse waveform is square and the pulse duration is 3.9 ns. As can be seen from Fig. 2(c), a stable pulse train with a period of 111 ns corresponds

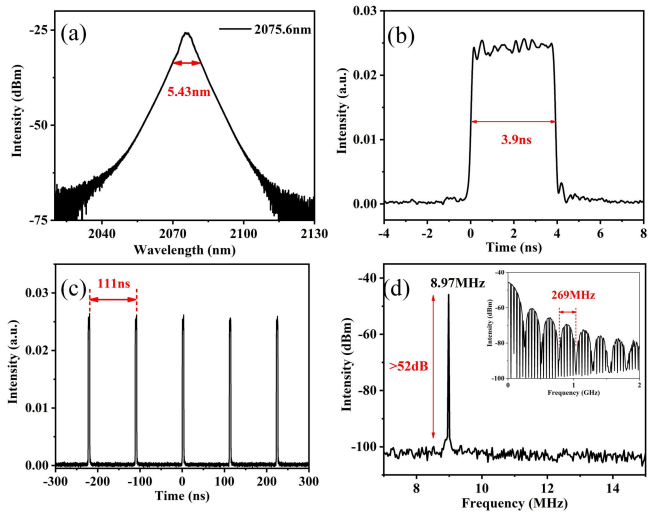

Fig. 2. Output characteristics of the DSR pulse. (a) Optical spectrum; (b)Single pulse; (c) Pulse train; (d) RF spectrum. Inset: RF spectrum in 2 GHz span.

to a 23 m long resonator. In addition, the RF spectrum is shown in Fig. 2(d) to evaluate the stability of the laser. It shows a signal to noise ratio (SNR) of 52 dB and the repetition rate of 8.97 MHz, indicating that the laser operates in fundamental mode-locking operation with very low-intensity noise. The inset in Fig. 2(d) shows a spectral modulation with a period of 269 MHz, corresponding to the duration of the pulse. Theoretically, the modulation frequency is the reciprocal of the duration of the corresponding pulse.

Then, the features of the DSR pulse at different pump power are analyzed at the fixed PCs orientation. The changing of spectrum with pump power is shown in Fig. 3(a). The same spectrum profile can be seen with the pump power from 1.35 to 2.1 W except for a marginally increase in intensity. The evolution process of single pulse is plotted in Fig. 3(b). Its characteristic is that the pulse duration broadens as the pump power increases, The pulse duration can be adjusted from 1.16 to 3.93 ns, whilst maintaining an almost constant intensity. As can be seen from Fig. 3(c), the SNR increases from 47 dB to 52 dB with the increase of the pump power from 1.35 W to 2.1 W. The 2D plot in insert of Fig. 3(c) further shows the RF traces with high overlaps, which means that the fundamental frequency is determined by the length of the cavity and is independent of the pump power. The modulating behavior on each RF trace can be clearly monitored in Fig. 3(d). Since higher pump power leads to wider pulse width, conversely, the lower modulation frequency is going to be.

In order to better exhibit the features of the DSR pulse, the relationship diagram is shown in Fig. 4. Fig. 4(a) and (b) show that average output power, pulse width, and pulse energy are all monotonically increasing with the pump power. When the pump power is 2.1 W, the output power is about 17.94 mW, the pulse energy can be calculated to be 2 nJ. At this time, the pulse width is 3.93 ns, so the corresponding peak power of DSR pulse can be calculated to be 508 mW, it almost maintains a stable value due to the peak-power-clamping (PPC) effect.

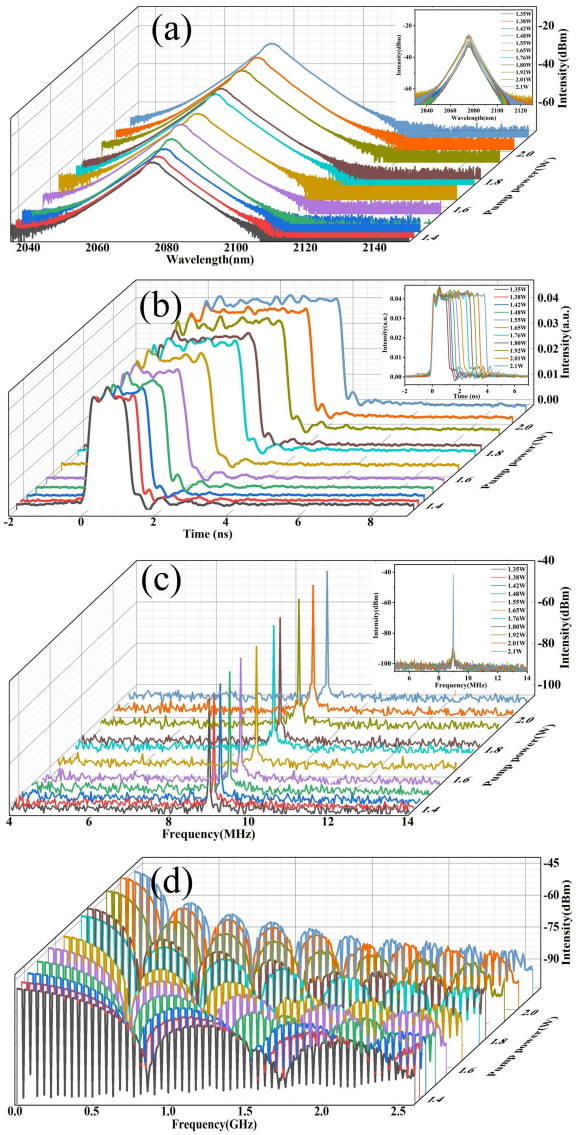

Fig. 3. Pump-power-related evolutions of DSR pulse (a) spectral profile of 2D and 3D; (b) pulse envelope of 2D and 3D; (c) the RF trace of 2D and 3D; (d) 2.5 GHz RF trace.

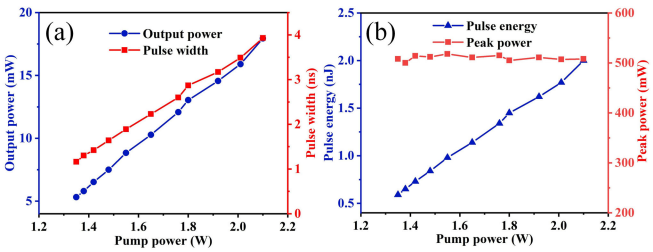

Fig. 4. (a) Output power and pulse duration versus the pump power; (b) Pulse energy and peak power versus pump powers.

Furthermore, DSR pulses operating at different wavelengths have also been found experimentally, despite the absence of any additional tunable filters in the cavity. As shown in Fig. 5, the tunable range of the wavelength is about 21.6 nm (from 2054.4 nm to 2076 nm) by properly adjusting PCs. This can be explained

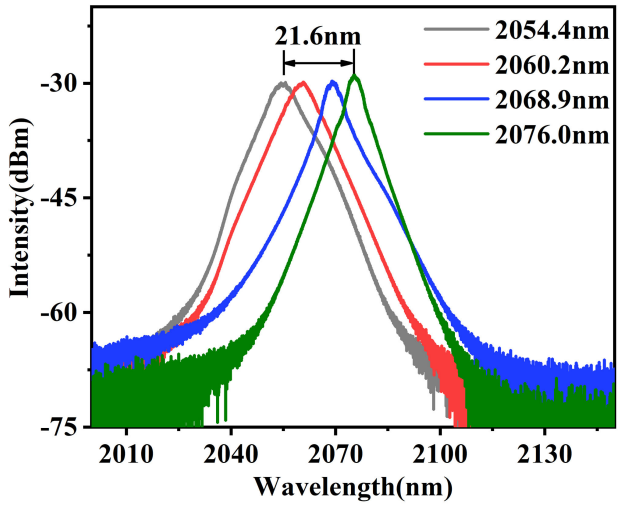

Fig. 5. Spectrum of DSR pulse at different wavelengths (from 2054.4 nm to 2076 nm).

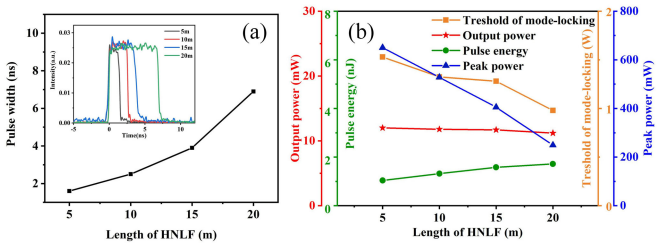

Fig. 6. Characteristics of DSR with the length of HNLF. (a) Pulse width; (b) Output power, pulse energy, threshold of mode-locking, and peak power with the length of HNLF.

by the transmission function of NALM: (1),

$$|T|^2 = 2\rho\,(1-\rho)\cdot(1+\cos\delta) \tag{1}$$

where T, ρ and δ represent the transmission, the split ratio of optical coupler and the phase difference in the opposite direction. Typically, total phase difference δ includes three parts, birefringent effect, the nonlinear effect, and the phase bias, shown in (2),

$$\delta = \Delta_{\text{birefringent}} + \Delta_{nl} + \Delta_{bias} \tag{2}$$

In the experiment, the mechanism of wavelength-selected can well be explained as different transmission functions correspond to different center wavelengths due to the different phase offset introduced by adjusting PCs.

Moreover, the nonlinear correlation characteristics of DSR laser are further explored by changing the 10 m long HNLF in the cavity with 5 m, 15 m and 20 m long HNLF, respectively. Fig. 6(a) illustrates that the pulse width can increase linearly with length of HNLF at the same pump power of 2.1 W. In detail, as depicted in the inset of Fig. 6(a), when the HNLF lengthened from 5 to 20 m, the pulse width can broaden from 1.6 to 6.9 ns. With the accumulation of the nonlinearity, the pulse mainly modulates by anti-saturation absorption, which will lead to a stronger PPC effect. Therefore, the transverse broadening

of the pulse will occur subsequently in time domain. Whereas the pulse top is still smooth for a longer HNLF. Another noted feature is that the threshold of mode-locking, decreases with the lengthening of HNLF, as shown in Fig. 6(b), because the increasing of nonlinearity of the cavity makes the mode-locking operation easier to realize. The output power is limited by pump power of 2.1 W, and the output powers with 5 m to 20 m long HNLF are similar due to the negligible transmission loss difference. According to the formula of output power and pulse width $P/f = P_0 \times \tau$, where P is output power, f is repetition frequency, P_0 is peak power and τ is pulse width, the result shown in Fig. 6(b) that the peak power decreases from 650 to 249 mW as the increasing of pulse energy from 1.04 to 1.72 nJ, which is due to the large tuning range of pulse width. In short, at the same pump power, it can be concluded that pulse width and pulse energy increase with the increasing of nonlinearity, and the threshold of DSR pulse can decrease. However, the peak power and output power are difficult to increase with the lengthening of HNLF. The peak power of the DSR pulse can be increased if the pulse is injected into the amplifier.

IV. Conclusion

In conclusion, we experimentally demonstrate an all-fiber DSR mode-locked holmium doped fiber laser with tunable wavelength and pulse width. For the DSR pulse operating at maximum pump power of 2.1 W, the pulse energy is up to 2 nJ. And the pulse width increases from 1.16 ns to 3.93 ns with the increasing of pump power. In addition, the pulse can operate in the wavelength range of 21.6 nm, from 2054.4 nm to 2076 nm by properly adjusting the PCs. By further lengthening the HNLF, it can be found that the longer HNLF, since the strong PPC effect, the larger the pulse width will occur subsequently, and the lower the peak power. This kind of fiber laser with wide wavelength-tunable range and high pulse energy has great potential in various applications.

References

[1] P. Lin, T. Wang, W. Ma, J. Chen, Z. Jiang, and C. Yu, "2-μm free-space data transmission based on an actively mode-locked holmium-doped fiber laser," *IEEE Photon. Technol. Lett.*, vol. 32, no. 5, pp. 223–226, Mar. 2020.

[2] P. Lin et al., "Propagation characteristics of 2.07 μm fiber laser in weak turbulence condition," *Opto-Electron. Eng.*, vol. 47, no. 3, 2020, Art. no. 190588.

[3] I. Mingareev, F. Weirauch, A. Olowinsky, L. Shah, P. Kadwani, and M. Richardson, "Welding of polymers using a 2 μm thulium fiber laser," *Opt. Laser Technol.*, vol. 44, no. 7, pp. 2095–2099, Oct. 2012.

[4] A. Hemming et al., "99 W mid-IR operation of a ZGP OPO at 25% duty cycle," *Opt. Exp.*, vol. 21, pp. 10062–10069, 2013.

[5] R. L. Blackmon, P. B. Irby, and N. M. Fried, "Comparison of holmium: YAG and thulium fiber laser lithotripsy: Ablation thresholds, ablation rates, and retropulsion effects," *J. Biomed. Opt.*, vol. 16, no. 7, 2011, Art. no. 071403.

[6] J. Wang, J. Han, J. He, C. Liao, and Y. Wang, "High-energy mode-locked holmium-doped fiber laser operating in noise-like pulse regime," *Opt. Lett.*, vol. 44, no. 18, pp. 4491–4494, Sep. 2019.

[7] W. Z. Ma et al., "Observation and optimization of 2 μm mode-locked pulses in all-fiber net anomalous dispersion laser cavity," *Opto-Electron. Adv.*, vol. 3, no. 11, Nov. 2020, Art. no. 200001.

[8] G. P. Agrawal, *Applications Nonlinear Fiber Optics*, 5th ed., Amsterdam, the Netherlands: Elsevier, 2013.

[9] B. Ibarra-Escamilla et al., "Dissipative soliton resonance in a thulium-doped all-fiber laser operating at large anomalous dispersion regime," *IEEE Photon. J.*, vol. 10, no. 5, Oct. 2018, Art. no. 1503907, doi: 10.1109/JPHOT.2018.2870572.

[10] W. Z. Ma et al., "Graphdiyne-decorated microfiber based soliton and noise-like pulse generation," *Nanophotonics*, vol. 10, no. 16, pp. 3967–3977, Oct. 2021.

[11] W. Chang, A. Ankiewicz, J. M. SotoCrespo, and N. Akhmediev, "Dissipative soliton resonances," *Phys. Rev. A*, vol. 78, no. 2, Aug. 2008, Art. no. 023830.

[12] W. Chang, J. M. Soto-Crespo, A. Ankiewicz, and N. Akhmediev, "Dissipative soliton resonances in the anomalous dispersion regime," *Phys. Rev. A*, vol. 79, no. 3, pp. 1039–1044, Mar. 2009.

[13] D. Edwin, G. Philippe, and K. J. Nathan, "Dissipative soliton resonance in a passively mode-locked fiber laser," *Opt. Lett.*, vol. 36, no. 7, pp. 1146–1148, Apr. 2011.

[14] L. Mei et al., "Width and amplitude tunable square-wave pulse in dual-pump passively mode-locked fiber laser," *Opt. Lett.*, vol. 39, no. 11, pp. 3235–3237, Jun. 2014.

[15] X. H. Li et al., "Wavelength-switchable and wavelength-tunable all-normal-dispersion mode-locked Yb-doped fiber laser based on single-walled carbon nanotube wall paper absorber," *IEEE Photon. J.*, vol. 4, no. 1, pp. 234–241, Feb. 2012.

[16] G. Krauss et al., "Compact coherent anti-Stokes Raman scattering microscope based on a picosecond two-color Er: Fiber laser system," *Opt. Lett.*, vol. 34,no. 18, pp. 2847–2849, Sep. 2009.

[17] D. Fu et al., "Probing skin pigmentation changes with transient absorption imaging of eumelanin and pheomelanin," *J. Biomed. Opt.*, vol. 13, no. 5, Sep. 2008, Art. no. 054036.

[18] A. A. Ivanov, M. V. Alfimov, and A. M. Zheltikov, "Wavelength-tunable ultrashort-pulse output of a photonic-crystal fiber designed to resolve ultrafast molecular dynamics," *Opt. Lett.*, vol. 31, no. 22, pp. 3330–3332, Nov. 2006.

[19] Z. L. Li, D. F. Jia, X. Sun, Z. Y. Wang, C. F. Ge, and T. X. Yang, "Wavelength-tunable square pulse generation based on dissipative soliton resonance," in *Proc. 8th Int. Conf. Opt. Commun. Netw.*, Anhui, China, 2019, pp. 1–3.

[20] J. H. Yang et al., "Observation of dissipative soliton resonance in a net-normal dispersion figure-of-eight fiber laser," *IEEE Photon. J.*, vol. 5, no. 3, Jun. 2013, Art. no. 1500806.

[21] X. Wang, Q. Liang, M. Sun, S. Yang, and S. Li, "Switchable operation of multiple solitons and dissipative soliton resonance in a C- and L-band mode-locked fiber laser," *Laser. Phys. Lett.*, vol. 17, no. 11, Nov. 2020, Art. no. 115103.

[22] H. Q. Lin, C. Y. Guo, S. C. Ruan, and J. H. Yang, "Dissipative soliton resonance in an all-normal-dispersion Yb-doped figure-eight fibre laser with tunable output," *Laser. Phys. Lett.*, vol. 11, no. 8, Jun. 2014, Art. no. 085102.

[23] Z. Zhang et al., "Wavelength and duration tunable dissipative soliton resonance fibre laser," *Laser Phys.*, vol. 30, no. 3, Feb. 2020, Art. no. 035103.

[24] S. L. Liu, Z. Y. Dou, B. Zhang, J. Hou, L. Y. Yang, and T. Y. Wu, "L-band wavelength-switchable dissipative soliton resonance Er-doped fiber laser," *IEEE Photon. J.*, vol. 12, no. 2, Apr. 2020, Art. no. 1501206.

[25] Y. F. Wu, J. R. Tian, Z. K. Dong, C. B. Liang, and Y. R. Song, "Generation of two dissipative soliton resonance pulses in an all-anomalous-dispersion regime thulium-doped fiber laser," *IEEE Photon. J.*, vol. 11, no. 6, Dec. 2019, Art. no. 1505308.

[26] W. Z. Ma et al., "1.9 μm square-wave passively Q-witched mode-locked fiber laser," *Opt. Exp.*, vol. 26, no. 10, pp. 12514–12521, May 2018.

[27] Y. Xu et al., "Dissipative soliton resonance in a wavelength-tunable thulium-doped fiber laser with net-normal dispersion," *IEEE Photon. J.*, vol. 7, no. 3, Jun. 2015, Art. no. 1502007.

[28] J. Zhao, L. Li, L. Zhao, D. Tang, and D. Shen, "Dissipative soliton resonances in a mode-locked holmium-doped fiber laser," *IEEE Photon. Technol. Lett.*, vol. 30, no. 19, pp. 1699–1702, Oct. 2018.

[29] J. Q. Zhao, L. Li, L. M. Zhao, D. Y. Tang, D. Y. Shen, and L. Su, "Dissipative soliton resonance and its depression into burst-like emission in a holmium-doped fiber laser with large normal dispersion," *Opt. lett.*, vol. 44, no. 10, pp. 2414–2417, May 2019.

[30] J. Zhao et al., "Nonlinear absorbing-loop mirror in a holmium-doped fiber laser," *J. Lightw. Technol.*, vol. 38, no. 21, pp. 6069–6075, Nov. 2020.